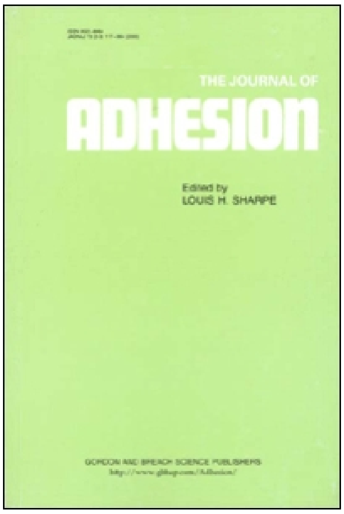

The Journal of Adhesion
Publication details, including instructions for authors and subscription information:
http://www.informaworld.com/smpp/title~content=t713453635

Surface Composition and Topography of Electrodeposited Polypyrrole Coatings on Steel Substrates

Wencheng Su[a]; Jude O. Iroh
[a] Department of Materials Science and Engineering, University of Cincinnati, Cincinnati, Ohio, USA

To cite this Article Su, Wencheng and Iroh, Jude O.(2000) 'Surface Composition and Topography of Electrodeposited Polypyrrole Coatings on Steel Substrates', The Journal of Adhesion, 73: 2, 215 — 231
To link to this Article: DOI: 10.1080/00218460008029307
URL: http://dx.doi.org/10.1080/00218460008029307

J. Adhesion, 2000, Vol. 73, pp. 215-231
Reprints available directly from the publisher
Photocopying permitted by license only

Published by license under
the Gordon and Breach Science
Publishers imprint.
Printed in Malaysia.

Surface Composition and Topography of Electrodeposited Polypyrrole Coatings on Steel Substrates*

WENCHENG SU and JUDE O. IROH[†]

Department of Materials Science and Engineering, University of Cincinnati, Cincinnati, Ohio 45221-0012, USA

(Received 11 October 1999; In final form 13 April 2000)

Polypyrrole coatings were successfully electrodeposited on low-carbon steel substrates from aqueous oxalate solutions. The surface composition and topography of the polypyrrole coatings formed under different conditions were investigated by X-ray photoelectron spectroscopy (XPS) and atomic force microscopy (AFM). The results show that the surface composition of the electrodeposited polypyrrole coatings basically reflects their bulk composition. Deposition of polypyrrole coatings on steel substrates also increased the surface roughness of the steel substrates.

Keywords: Polypyrrole; Steel; Surface composition; Surface topography

1. INTRODUCTION

Polymer coatings are currently the most widely used method for prevention of metallic corrosion, however, traditional coating techniques often require the use of the toxic chemicals such as chromate and volatile organic compounds [1, 2]. Due to environmental concern, industries are now looking for effective and environmentally-favorable

---

*One of a Collection of papers honoring F. James Boerio, the recipient in February 1999 of *The Adhesion Society Award for Excellence in Adhesion Science, Sponsored by 3M.*

[†] Corresponding author. Tel.: 513-556-3115, Fax: 513-556-2569, e-mail: jiroh@uceng.uc.edu

coating processes. In recent years, the electrodeposition of polypyrrole coatings on iron or steel substrates has been investigated for the purpose of corrosion protection [3–11]. The electrodeposited polypyrrole coatings are usually very thin coatings on steel substrates (several microns). For efficient corrosion protection, application of top coatings is generally necessary. The adhesion between the electrodeposited coating and top coating is a very important factor in determining the overall performance of the coating system. The adhesion between two substances is influenced significantly by the chemical and morphological nature of their surfaces. In this paper, the surface composition and topography of the electrodeposited polypyrrole coatings were investigated by X-ray photoelectron spectroscopy (XPS) and atomic force microscopy (AFM). The purpose of these investigations is to provide important information for the application of strongly adherent top coatings.

2. EXPERIMENTAL

2.1. Electrochemical Synthesis

Pyrrole and tetrachloroethylene were Aldrich products while sodium bicarbonate was purchased from Fisher Scientific. The aqueous solutions were all made from deionized water obtained from a Labconco Water Pro PS System. QD low carbon steel panels were provided by Q-panel Company, Ohio. The received panels already had a good surface finish (roughness less than 0.2 µm) and were used without further polishing, but they were degreased with tetrachloroethylene for about an hour prior to the electrochemical reactions.

Electrochemical reactions were performed in a one-compartment polypropylene cell. The steel working electrode was fixed in the center of the cell by a polypropylene frame so that both sides of the sheet could be coated. The counter electrodes comprised two titanium alloy plates. A saturated calomel electrode (SCE) was used as the reference electrode. A constant current method was the technique used in this research work. The constant current source was supplied by an EG&G

Princeton Applied Research Potentiostat/Galvanostat Model 273A. The initial pyrrole concentration was kept constant at 0.25 M. The electrolyte used was a mixture of oxalic acid and $NaHCO_3$. $NaHCO_3$ was used to adjust the pH of the solutions. The concentration of the electrolyte was kept constant at 0.1 M. After each reaction, the obtained sample was rinsed with deionized water and acetone and dried in vacuum oven at 65°C to constant weight.

2.2. X-ray Photoelectron Spectroscopy (XPS)

A Perkin–Elmer Model 5300 XPS spectrometer with Mg $K\alpha$ X-rays, operating at 300 W and 15 kV DC, was used to obtain XPS spectra. An Apollo computer system with Perkin–Elmer software was used for data acquisition and processing. XPS spectra were recorded at take-off angles of 45°. The take-off angle was defined as the angle between the sample surface and the direction of propagation of the exiting photoelectrons. Surface elemental stoichiometries were obtained from peak area ratios corrected with the appropriate experimentally-determined elemental sensitivity factors. The carbon 1s (C1s), oxygen 1s (O1s), and nitrogen 1s (N1s) spectra were fitted to Gaussian component peaks of equal full-width at half-maximum (FWHM). The position and intensity of the component peaks were optimized to give the best fit to the experimental spectrum. The binding energies are quoted relative to hydrocarbon C1s at 285.0 eV.

2.3. Atomic Force Microscopy (AFM)

A Burleigh Metris 2000 Atomic Force Microscope was used to get the image of the electrodeposited coatings. The as-prepared sample was fixed on the sample holder by double-sided tape. The microscope was run in the constant force mode. Silicon nitride tips, integrated on a 100 μm silicon nitride cantilever (spring constant 0.098 N/m), were used. The force between the tip and the sample was about 0.5 nN. For the construction of each image, an area of 25 μm × 25 μm was scanned. The images were acquired at various magnifications as indicated in the respective figures.

3. RESULTS AND DISCUSSION

3.1. Surface Composition

X-ray photoelectron spectroscopy (XPS) was used to study the surface composition of the electrodeposited coatings. XPS is one of the most powerful surface-sensitive techniques with a sampling depth less than 100 Å. In addition to its surface sensitivity, XPS is also uniquely capable of providing chemical information such as oxidation state and chemical bonding, as well as elemental compositions [12]. For XPS, the sampling depth is, in fact, limited by inelastic scattering events which are characterized by the inelastic mean free path, λ, of the photoelectrons. Since approximately 95% of the signal intensity is derived from a distance 3λ within the solid, the sampling depth, d, as a function of the angle θ of electron exit relative to the sample surface (take-off angle), is usually taken to be [13]

$$d = 3\lambda \sin\theta \tag{1}$$

Assuming that the inelastic mean free path, λ, of the C1s photoelectrons in organic compounds is 27 Å [12], the sampling depth is estimated to be about 57 Å at a 45° take-off angle.

As shown in Figure 1, the formation process of polypyrrole coatings was different between acidic and basic solutions [10, 11]. In basic solutions, the passivation of steel was established immediately after the current was supplied. In acidic solutions, however, the formation process of polypyrrole coatings was characterized by two distinct stages. After the passivation of steel was established at the end of the first stage, the reaction potentials were raised to the electropolymerization potentials of pyrrole and black polypyrrole coatings were deposited on the steel substrates during the second stage. Our previous results have shown that the passivation of the steel substrate was due to the deposition of an iron(II) oxalate dihydrate coating, which was composed of a monolayer of closely-packed, small crystals [11]. The electrochemical reactions can be expressed by following two equations:

$$\mathrm{Fe} + 2\mathrm{e} \longrightarrow \mathrm{Fe}^{2+} \tag{1}$$

$$\mathrm{Fe}^{2+} + \mathrm{C_2O_4^{2-}} + 2\mathrm{H_2O} \longrightarrow \mathrm{FeC_2O_4} \cdot 2\mathrm{H_2O} \tag{2}$$

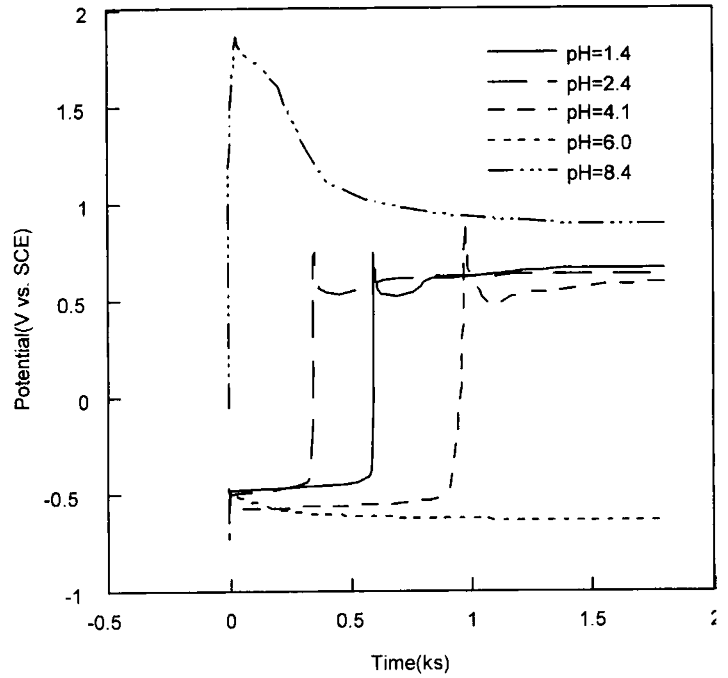

FIGURE 1 Potential-time curves for the formation of polypyrrole coatings in different pH solutions at the applied current density of 0.56 mA/cm^2.

The deposition process of the iron(II) oxalate dihydrate on the steel substrate involves two steps: nucleation and growth. The effect of solution pH on the deposition process is not yet well understood. Perhaps solution pH has a great effect on the nucleation rate of the iron(II) oxalate. For this system, nucleation will occur on the steel substrate when the solubility of $FeC_2O_4 \cdot 2H_2O$ is reached.

Although the solubility of the $FeC_2O_4 \cdot 2H_2O$ is very small in pure aqueous solution, solution pH might influence the solubility of $FeC_2O_4 \cdot 2H_2O$. It has been reported that iron(II) oxalate can convert into soluble complexes, $M_2[Fe(C_2O_4)_2]$, in the presence of excess alkali metal oxalate [11]. Perhaps the solubility of the $FeC_2O_4 \cdot 2H_2O$ is smallest in the medium of $pH = 2.4$, resulting in a higher nucleation rate. The solubility of $FeC_2O_4 \cdot 2H_2O$ might be very high in the medium of $pH = 6.0$, thus, it would take a very long time for nucleation to occur on the substrate surface.

Studying the surface composition of the bare steel substrate and the iron(II) oxalate coatings should help to understand the surface change during the reactions. The surface composition of the polished steel substrate (polished by abrasive paper followed by acetone cleaning) was analyzed by XPS. The obtained relative atomic concentrations of the elements present on the steel surface are listed in Table I. It can be seen that there is a large amount of adsorbed organic contaminants on the steel surface. XPS also shows the presence of Si on the steel surface which probably came from the abrasive paper used during the polishing process.

Three iron(II) oxalate dihydrate coatings formed in the solutions with $pH = 1.4$, 2.4 and 4.1 were also analyzed by XPS. The surface atomic concentrations of these coatings are also listed in Table I. It can be seen that the surface composition of these three coatings is very similar. Considering only Fe, C and O elements in the iron(II) oxalate dihydrate, the theoretical relative atomic concentrations are calculated as the following: Fe: 11.11%, C: 22.22%, and O: 66.66%. It is very clear that the surface composition of the iron(II) oxalate coatings is different from their bulk composition. The surface content of oxygen is much lower than its corresponding bulk content while the surface content of carbon is much higher than its bulk content. This implies that the iron(II) oxalate coatings also adsorb a large amount of hydrocarbon contaminants on their surfaces. It can be seen from Table I that a very small amount of nitrogen is detected on the surface of iron(II) oxalate coatings, which might come from the adsorbed pyrrole.

A passive film was also prepared in the solution of $pH = 8.4$, to which no pyrrole monomer was added. The electrochemical reaction

TABLE I XPS atomic concentrations of the polished steel and passive film and coatings

	Atomic concentration (%)				
Sample	*C1s*	*O1s*	*Fe2p*	*N1s*	*Si2p*
Polished Steel	71.2	23.2	1.6		4.0
$FeC_2O_4 \cdot 2H_2O$, $pH = 1.4$	47.9	45.8	6.2	0.1	
$FeC_2O_4 \cdot 2H_2O$, $pH = 2.4$	47.0	46.3	6.1	0.6	
$FeC_2O_4 \cdot 2H_20$, $pH = 4.1$	51.8	42.3	5.4	0.5	
Iron Oxide, $pH = 8.4$	58.0	34.1	4.8	3.1	
Polypyrrole, $pH = 1.4$	77.8	12.0		10.2	

was stopped immediately when the reaction potential reached 1.0 V. The obtained sample was then rinsed thoroughly with deionized water and acetone and dried in a vacuum oven. The measured XPS atomic concentrations are also listed in Table I. A small amount of nitrogen is detected on the sample surface. The source of this element is not very clear, maybe it resulted from the handling process. Compared with the bare steel, the carbon content was decreased while the oxygen content was increased.

For the three iron(II) oxalate coatings, the C1s and O1s spectra were further deconvoluted into component peaks. It is found that the component peaks for each element are very similar among these three coatings. As an example, only the curve-fitted C1s and O1s spectra for the iron(II) oxalate coating formed at pH = 1.4 are shown in Figure 2. Deconvolution of the C1s signal leads to three main components, at 285.0, 286.8, and 289.0 eV with relative intensities 56:9:35. The three components can be attributed to C—C, C—N/C—O, and O=C—O groups, respectively [14, 15]. The C—C and C—N/C—O groups come from the organic contaminants while the O=C—O groups should come from the iron(II) oxalate. The O1s signal can be decomposed into three components, at 531.0, 532.4 and 533.7 eV, with relative intensities close to 9:74:16. The three components correspond to OH, O=C—O and H_2O, respectively [16–17]. According to the structure of $FeC_2O_4 \cdot 2H_2O$, the two oxygen atoms of the O=C—O groups are basically equivalent. OH might come from organic contaminants, while O=C—O and H_2O should mainly come from the iron(II) oxalate coatings.

The curve-fitted C1s and O1s spectra for the passive film formed in basic solution are shown in Figure 3. The C1s spectrum is deconvoluted into four component peaks, at 285.0, 286.2, 287.4 and 288.5 eV, with relative intensities close to 84:4:3:9. The four component peaks can be assigned to C—C, C—O/C—N, C=O and O=C—O groups [14, 15]. It can be seen that carbon on the film surface is dominated by the hydrocarbon contaminants. Curve-fitting of the O1s spectrum revealed three component peaks, located at 530.1, 531.8 and 533.3 eV, with relative intensities close to 39:49:12. The three component peaks can be assigned to O^{2-} (iron oxides), C=O (from acetone) or $\underline{O}$=C—O (from oxalate), and O=C—$\underline{O}$ groups (from oxalate) [18, 19]. Based on the above results, it can be concluded

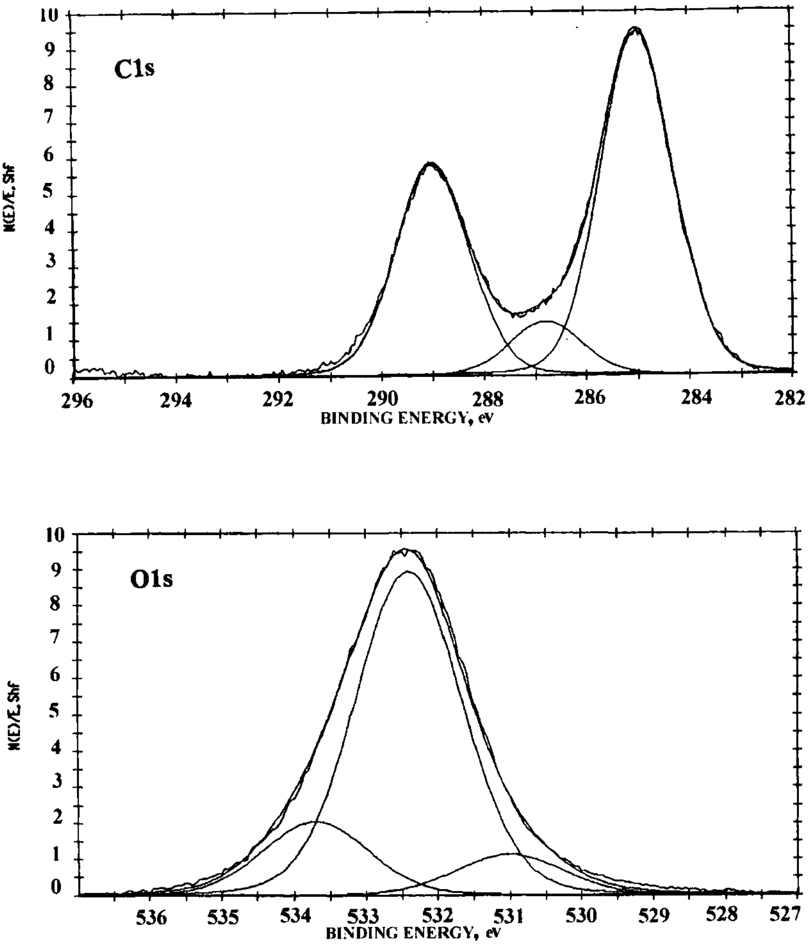

FIGURE 2 Curve-fitted C1s and O1s spectra for the iron(II) oxalate formed at pH = 1.4.

that the surface of the passive film formed in basic solution mainly consists of iron oxide (Fe_2O_3, Fe_3O_4...) and some adsorbed organic contaminants. The above results are not unusual. According to a Pourbaix diagram, the application of an anodic potential to an iron sheet immersed in basic solution will result in the formation of a passive iron oxide film [1, 3, 4].

Figure 4 shows the XPS survey spectrum of the polypyrrole coating formed at pH = 1.4 and an applied current density of 0.56 mA/cm^2 for

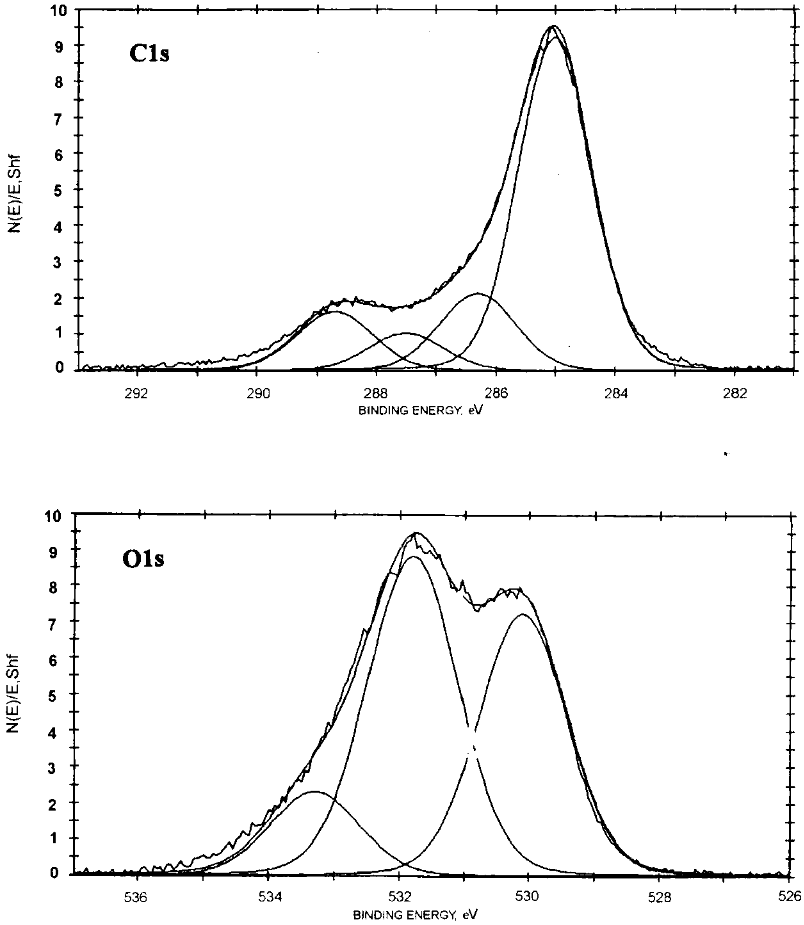

FIGURE 3 Curve-fitted C1s and O1s spectra for the passive film formed in basic solution.

30 min. For this sample, no iron is detected, indicating that the steel substrate was completely covered by the polypyrrole coating, which had been demonstrated previously by the SEM results [11]. As shown in Table I, XPS analysis of the polypyrrole coating shows the presence of C(77.81%), N(10.22%) and O(11.98%). Only considering C, N, and O in the bulk polypyrrole, the relative atomic concentrations can be calculated from the results of elemental analysis, which shows 68% C, 17% N and 15% O. It can be seen that the surface elemental

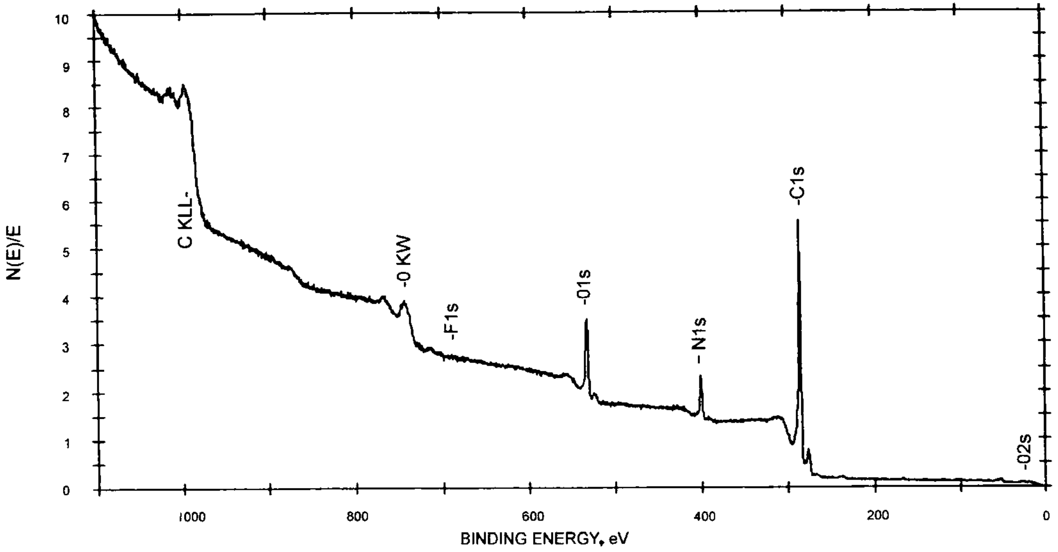

FIGURE 4 XPS survey spectrum of the polypyrrole coating, pH = 1.4, $i = 0.56\,\mathrm{mA/cm^2}$.

composition of polypyrrole is very similar to its bulk composition. Of course, a small amount of hydrocarbon contaminants must be adsorbed on the surface.

Figure 5 shows the curve-fitted C1s, N1s and O1s spectra for the polypyrrole coating. The C1s spectrum shows four component peaks, at 285.0, 286.6, 287.8 and 289.0 eV, with relative intensities 73 : 14 : 8 : 5. The peaks at 285.0 and 286.6 eV can be attributed to C—C and C—N/C=N groups, respectively. Most C—C and C—N/C=N should come from the pyrrole units. The peak near 287.8 eV results from C=O groups which might come from residual organic contaminants (acetone) and surface overoxidation of polypyrrole. The surface overoxidation of polypyrrole has also been reported by other authors [20]. The component around 289.0 eV can be attributed to O=C—O groups [14, 15], which should come from the hydrogen oxalate counterions.

The N1s signal is composed of three components,centered at 398.4, 400.2 and 402.2 eV, with relative intensities close to 14 : 73 : 12. The lower and higher binding energy shoulders have similar intensities. This feature of the N1s spectrum for electrochemically-prepared polypyrrole was also observed by other authors [20–25]. The main central peak corresponds to neutral pyrrole nitrogen. The high binding energy shoulder can be assigned to nitrogen atoms present in the vicinity of the charged site on the polymer. Accordingly, positive

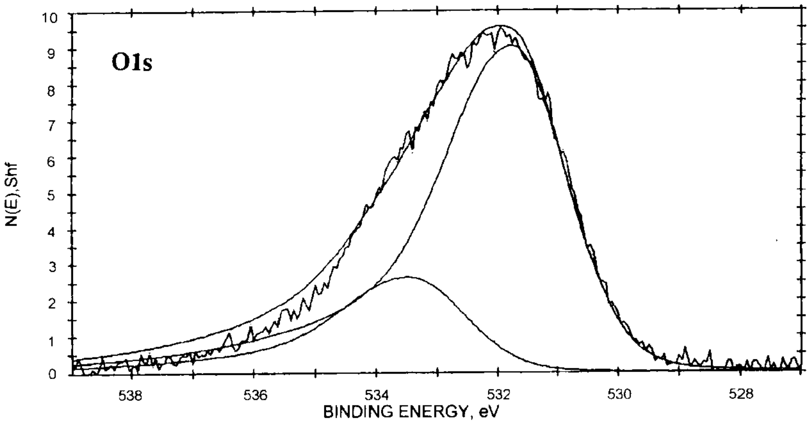

FIGURE 5 Curve-fitted C1s, N1s and O1s spectra for the polypyrrole coating.

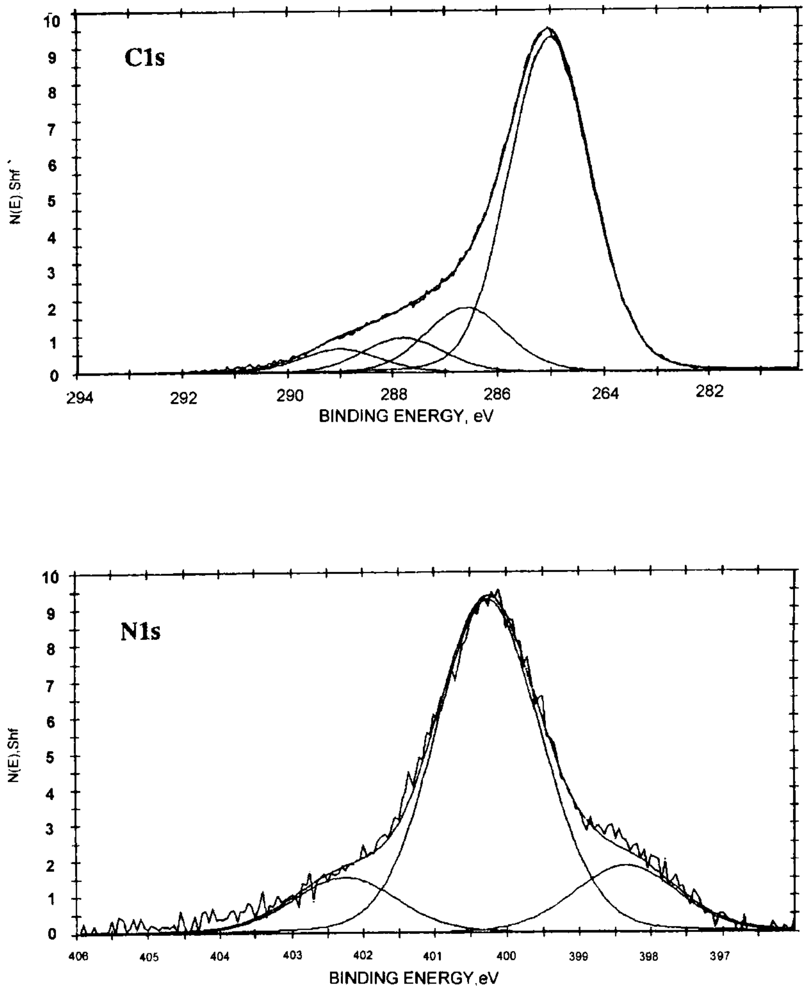

FIGURE 5 (Continued).

charge delocalization over several atoms can result in increased charge on the nitrogen atom, which has been postulated to range from one-sixth to a single charge. There are some discrepancies in the assignment of the lower binding energy shoulder in the literature, but most authors believe that the lower binding energy shoulder might be due to deprotonation of a certain fraction of the pyrrole nitrogen, followed by rearrangement of the pyrrole bonds to satisfy the three nitrogen valencies, resulting in an electron-rich surrounding of the nitrogen [21–24].

The O1s signal is quite broad and can be decomposed into two components at 531.7 and 533.4 eV, with relative intensities close to 63 : 37. The peak around 531.7 eV probably comes from C=O and $\underline{O}=C{-}O$ groups while the peak around 533.4 eV can be attributed to $O=C{-}\underline{O}$ groups [18, 19, 21]. The O=C—O groups mentioned above should mainly come from the hydrogen oxalate counterions. The C=O groups might come from residual organic contaminants (acetone) and overoxidation of polypyrrole.

As discussed above, XPS analysis shows that there are some functional groups on the polypyrrole coating's surface, such as carboxyl and N—H groups. These functional groups can significantly promote the adhesion through the formation of hydrogen bonding and even chemical bonding. Interfacial chemical bonding can increase the adhesive bond strength by, (i) preventing molecular slippage at a sharp interface during fracture, and (ii) increasing the fracture energy by increasing the interfacial attraction.

3.2. Surface Topography

Surface topography of the electrodeposited polypyrrole coatings was investigated by atomic force microscopy (AFM). AFM is one of the most sensitive tools for investigating surface topography and it is well suited to study the surface topography of organic surfaces [26].

For AFM investigation, all samples were prepared by using the same electropolymerization charge per unit area. According to weight measurement, the thickness of the polypyrrole coatings formed under different conditions is around 2.5 μm. Figure 6 shows the AFM image of the unpolished bare steel surface while Figure 7 shows the AFM image of the polypyrrole coating formed at pH = 2.4 and 1.13 mA/cm^2. It can be seen clearly that the original steel surface is relatively featureless and smooth. The deposition of the polypyrrole coating on the steel substrate led to the formation of microspheroidal features. The results of AFM are consistent with those of SEM, which had revealed a very uniform surface of the electrodeposited polypyrrole coatings [8, 10]. The AFM scans at several

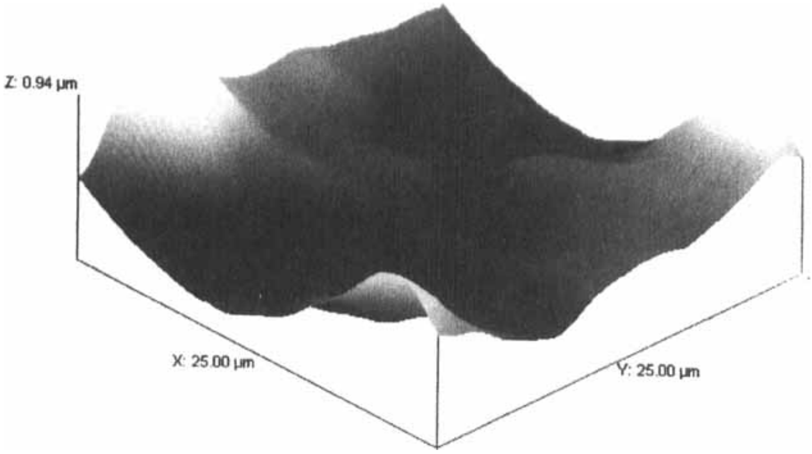

FIGURE 6 AFM image of the unpolished bare steel surface. (See Color Plate I).

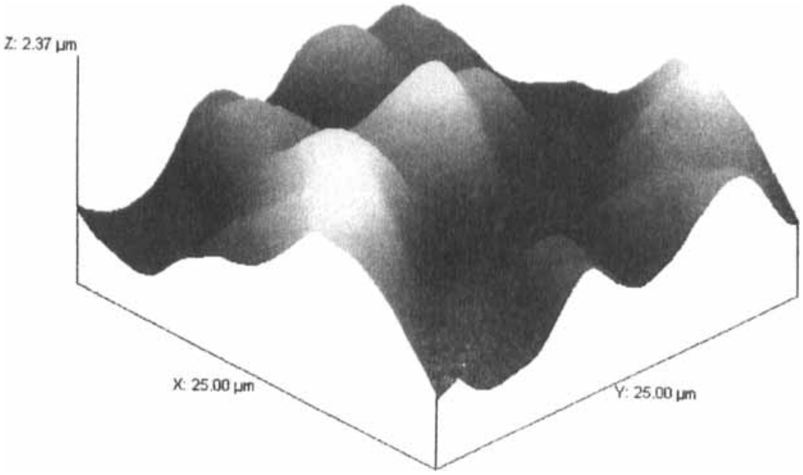

FIGURE 7 AFM image of the polypyrrole coating formed at $pH = 2.4$ and $i = 1.13\,mA/cm^2$. (See Color Plate II).

different spots of the same sample also showed very similar surface topography.

The studies on surface topography can also lead to some information about the surface roughness of the electrodeposited coatings. The mean roughness of the surface, R_a, is defined by

TABLE II Mean roughness of the electrodeposited polypyrrole coatings

Sample	*Ra* (μm)
Bare steel	0.12
PPy, pH = 1.4, $i = 1.13\,\mathrm{mA/cm^2}$	0.37
PPy, pH = 2.4, $i = 1.13\,\mathrm{mA/cm^2}$	0.34
PPy, pH = 4.1, $i = 1.13\,\mathrm{mA/cm^2}$	0.31
PPy, pH = 2.4, $i = 1.13\,\mathrm{mA/cm^2}$	0.34
PPy, pH = 2.4, $i = 3.38\,\mathrm{mA/crn^2}$	0.45

following equation:

$$R_a = 1/N(\Sigma|Z_i - Z_{\mathrm{avg}}|) \tag{2}$$

where Z_i is the height of a point on the surface and Z_{avg} is the average height of all the points on the surface. The determined R_a values for the bare steel and the electrodeposited polypyrrole coatings are listed in Table II.

Because AFM is capable of measuring the height of a point on the surface to the accuracy of 0.01 μm, it is possible to compare the surface roughness for the samples formed at different conditions. It can be seen that the steel surface was made rougher after the deposition of polypyrrole coatings. For example, the surface roughness values increased from 0.12 μm for the bare steel substrate to 0.37 μm for the polypyrrole coating formed at pH = 1.4 and $1.13\,\mathrm{mA/cm^2}$. For the same applied current density, a slight decrease in roughness with pH was found for the polypyrrole coatings formed at pH below 4.1. It is also very clear that the surface roughness of the polypyrrole coatings also increased with increasing applied current density for solutions with the same pH. Mechanical interlocking is regarded as one of the most important mechanisms for strong bonding. The increased roughness of the surface of the polypyrrole coatings can provide numerous interlocking sites, which will also significantly improve the adhesion between the electrocoated steel substrates and the top coatings.

4. CONCLUSIONS

The results of XPS show that the electrodeposited polypyrrole coatings completely covered the steel substrates. The surface composition of the polypyrrole coatings basically reflects their bulk composition. Deposition of polypyrrole coatings on steel substrates also led to increases in the surface roughness of the steel substrates. The surface roughness of the electrodeposited polypyrrole coatings was influenced by the electrochemical processing parameters. The surface chemistry and surface topography of the electrodeposited polypyrrole coatings are all favorable for the application of strongly adherent top coatings. It would be very interesting to evaluate further the overall performance of the electrodeposited polypyrrole/topcoating systems.

Acknowledgment

The financial support from the Office of Naval Research is gratefully acknowledged.

References

[1] Jones, D. A., *Principles and Prevention of Corrosion* (Macmillan Publishing Company, New York, 1992).

[2] Homes, J., *Metal Finishing* **87**(11), 65 (1989).

[3] Cheung, K. M., Bloor, D. and Stevens, G. C., *Polymer* **29**, 1709 (1988).

[4] Ferreira, C. A., Aeiyach, S., Delamar, M. and Lacaze, P. C., *J. Electroanal. Chem.* **284**, 351 (1990).

[5] Schirmeisen, M. and Beck, F., *J. Appl. Electrochem.* **19**, 401 (1989).

[6] Beck, F. and Michaelis, R., *J. Coatings Technology* **64**(808), 59 (1992).

[7] Beck, F., Michaelis, R., Schloten, F. and Zinger, B., *Electrochimica Acta* **39**, 229 (1994).

[8] Su, W. and Iroh, J. O., *J. Appl. Polym. Sci.* **65**(3), 417 (1997).

[9] Su, W. and Iroh, J. O., *J. Appl. Polym. Sci.* **65**(3), 617 (1997).

[10] Su, W. and Iroh, J. O., *Synth. Met.* **95**(3), 159 (1998).

[11] Iroh, J. O. and Su, W., *J. Appl. Polym. Sci.*, **71**(12), 2075 (1999).

[12] *Handbook of X-ray Photoelectron Spectroscopy*, Chastein, J. Ed. (Perkin-Elmer Corp., Eden Prairie, Minnesota, 1992).

[13] Seah, M. P. and Dench, W. A., *Surf. Interface Anal.* **1**, 1 (1979).

[14] Clark, D. T. and Dilks, A., *J. Polym. Sci., Polym. Chem. Ed.* **16**, 991 (1978).

[15] Clark, D. T. and Dilks, A., *J. Polym. Sci., Polym. Chem. Ed.* **17**, 957 (1979).

[16] Clark, D. T. and Thomas, H. R., *J. Polym. Sci., Polym. Chem. Ed.* **16**, 791 (1978).

[17] Clark, D. T. and Harrison, A., *J. Polym. Sci., Polym. Chem. Ed.* **19**, 1945 (1981).

[18] Mazurkiewicz, B., *Electrochimica Acta* **38**(4), 495 (1993).

[19] Kurbatov, G. G., Darque-Ceretti, E. and Aucouturier, M., *Surf. Interface Anal.* **12**, 811 (1992).

[20] Vigmond, S. J., Kallury, K. M. R. and Thompson, M., *Anal. Chem.* **64**, 2763 (1992).

[21] Skotheim, T. A., Florit, M. I., Melo, A. and O'Grady, W. E., *Phys. Rev. B.* **30**, 4846 (1984).

[22] Ingans, O., Erlandsson, R., Nylander, C. and Lundstrm, I., *J. Phys. Chem. Solids* **45**(4), 427 (1984).

[23] Erlandsson, R., Ingams, O., Lundstrm, I. and Salaneck, W. R., *Synth. Met.* **10**, 303 (1985).

[24] Eaves, J. G., Munro, H. S. and Parker, D., *Polymer Communications* **28**, 38 (1987).

[25] Vigmond, S. J., Kallury, K. M. R., Ghaemmaghami, V. and Thompson, M., *Talanta* **39**(4), 449 (1992).

[26] *Encyclopedia of Materials Characterization: Surfaces, Interfaces, Thin Films*, Brundle, C. R., Evans, C. A. Jr. and Wilson, S. Eds. (Butterworth–Heinenann, Stoneham, MA, 1992).